



Impact of sodium ion impregnation on the photocatalytic hydrogen evolution activities of anatase/rutile mixed phase TiO₂ nanomaterials

Sruthy Raj P^a, Prathyusha K R^a, Resmi M R^b, Sreenivasan Koliyath Parayil^{a,*}

^aUniversity of Calicut Approved Research Centre in Chemistry, MES Kalladi College, Mannarkkad 678 583, Kerala, India

^bPG & Research Department of Chemistry, SNGS College, Pattambi 679 306, Kerala, India

*E-mail: drsreenivasan@meskc.ac.in

Received 06 July 2020; revised and accepted 18 August 2021

Sodium ion impregnated anatase/rutile mixed phase TiO₂ material has been synthesised by sol-gel method and characterised for understanding the solar hydrogen production activities. The presence of sodium ion can influence the crystallinity, crystallite size and photocatalytic efficiency of mixed phase TiO₂. The hydrogen evolution activities of the sodium impregnated TiO₂ and bare TiO₂ materials are compared by calculating the yield of H₂ gas evolved from the dissociation of H₂O. Even though the presence of rutile/anatase mixed phase TiO₂ is suitable for hydrogen evolution under UV/visible light irradiation, it is found that bare TiO₂ can act as a good catalyst and gives a hydrogen evolution value of 134 μmol after 5 h of irradiation from 20 mg of the catalyst. However, the sodium impregnated TiO₂ material show lower hydrogen evolution as compared to bare TiO₂ and a value of 34 μmol under similar experimental condition. The variation in hydrogen evolution may be exhibited due to high crystallinity, large crystallite size and higher percentage of the rutile phase in bare TiO₂ compared to sodium impregnated TiO₂ material. This study will be helpful for understanding the effect of alkali metal ion in metal oxide semiconductor and further understanding their detrimental effect on photocatalytic water splitting and related applications.

Keywords: Sol-Gel synthesis, Impregnation, Na⁺ modified TiO₂, Photocatalysis, Water splitting

Transition metal oxide nanomaterials are an exciting area of research due to the utilization of abundant renewable resources for a wide variety of applications such as dye sensitized solar cell^{1,2} remediation of environmental contaminants³⁻⁶, clean energy production through environmental friendly methods, bio sensing of molecules⁹ and artificial light harvesting¹⁰⁻¹². The generation of hydrogen from water in the presence of a metal oxide provides a new platform through which energy costs and environmental pollution can be reduced. Even though TiO₂ is an ideal for energy production, the absorption of energy from sunlight and generation of hydrogen is still a challenging project. This process requires a chemically stable, non-toxic visible light photocatalyst that can be prepared by highly economical way and control the electron-hole recombination¹³. The absorption of wide band gap semiconductor limited to the application in the UV region, extensive research has demonstrated the ability of this semiconductor to absorb photons of light and generate excitons that migrate to the surface of the photocatalyst and take part in oxidation and reduction reaction¹⁴⁻¹⁵. In light activated water splitting, extended life time of the electrons is vivacious to enable the reduction of

hydrogen ions. However, the fast decay of electrons causes recombination of charge carriers, which further diminishes the photocatalytic efficiency of the semiconductor¹⁶.

Several approaches have been investigated for the modification of the semiconductor metal oxide using metal ions and improve the life time of the electrons and holes¹⁷⁻²². Parayil *et al.* reported the photocatalytic hydrogen generation from carbon modified anatase/rutile nanomaterials²³⁻²⁴. Yung *et al.* synthesized mixed phase anatase/rutile nanomaterial for water splitting and reported the synergistic effect in such mixed phase system²⁵. Even though transition metal cation doped TiO₂ was explored well²⁶⁻²⁸ the alkali or alkaline earth metal modified TiO₂ was not explored well in photocatalytic applications. The reported results mainly focused on adsorption and degradation studies. Xie *et al.* reported the influence of sodium ion in photocatalytic efficiency²⁹. Guillard *et al.* reported the decrease in photocatalytic activity of TiO₂ in presence of sodium ion³⁰. Ivan *et al.* reported the adsorption ability of sodium ion modified TiO₂³¹. Zhibiao *et al.* reported the influence of alkali metal ion on CO₂ hydrogenation³². Nam *et al.* reported the influence of sodium ion in photocatalytic activity³³. In most of

the reported article sodium has a detrimental effect on visible light photocatalysis. The influence of sodium ion in photocatalytic water splitting was recently reported by Parayil *et al.*³⁴. However their study focused on rutile TiO₂. Moreover the synthesis procedure was slightly different from current work. In this manuscript, we attempted to understand the effect of sodium ion impregnation on the mixed phase TiO₂ nanomaterial and its influence in photocatalytic hydrogen generation.

Materials and Methods

Commercially available titanium tetraisopropoxide, (97%, Sigma Aldrich, USA), denatured ethanol, conc. HNO₃ (Nice Chemicals), sodium chloride (Nice Chemicals) were used as received. Deionized water was used throughout the experiments. For the synthesis of mixed phase TiO₂ xerogel²³, Typically 11 mL of titanium isopropoxide was added drop wise to a solution containing 90 mL of denatured ethanol under vigorous stirring in a beaker. The hydrolysis process was initiated by the addition of 5 mL water and catalyzed by addition of 500 μ L conc. HNO₃. The resulting mixture was stirred for 3 h to obtain a wet gel. The obtained product kept for drying at room temperature. After drying it is subjected to calcinations at 550 °C for 6 h in a muffle furnace under static air environment.

For studying the influence of sodium ions on the formation, structure and photocatalytic activity of TiO₂ xerogel, sodium impregnated TiO₂ xerogel was prepared. About 0.3 g of TiO₂ xerogel material was added to a solution containing 9 mL denatured ethanol. 500 μ L of 2% NaCl was added along with 100 μ L of conc. HNO₃. The obtained mixture was aged for 3 h at room temperature. This leads to the formation of a wet gel through condensation process. The wet gel was finally converted into a dry gel after drying at ambient atmosphere. The resultant material was further calcined at 550 °C for 6 h in a muffle furnace at a heating rate of 10° per min. under static air atmosphere. The obtained powdered material was labeled as Na impregnated TiO₂.

Material characterization

The synthesized materials were characterized by powder X-ray diffraction, UV-visible diffuse reflectance spectroscopy (DRS), Raman spectroscopic analysis and transmission electron microscopy (TEM). The powder XRD measurements were performed at room temperature on a Bruker AXS D8

advance diffractometer using Cu-K α radiation ($\lambda=1.5406$ Å) and the samples were scanned with a step size of 0.02 at a scan speed of 1°/min in the range of $2\theta=10$ to 80°. The FT-Raman measurements using 1064-nm excitation were performed on a Bruker MultiRAM FT-Raman spectrometer equipped with an InGaAs detector operating at 0.8 cm⁻¹ resolution and power ranging from 0.5 to 1.0 W. The UV-visible diffuse spectra were recorded on a Jasco V-750 UV-visible spectrophotometer. The TEM measurement was done by using Jeol/JEM 2100 of voltage 200 kV is capable of a spatial resolution of 0.14 nm and LaB₆ is used as the source of radiation.

Photocatalytic water splitting studies

The role of Na⁺ ions impregnation on TiO₂ material was studied by carrying out the UV-visible light photocatalytic hydrogen evolution studies of the synthesised materials. The experiment was performed in a stainless steel reactor with a side cavity. Methanol was used as the sacrificial reagent. Typically, 20 mg of the material was suspended in 50 mL solution containing H₂O and methanol in a 4:1 ratio. The suspension was degassed for 30 min with high-purity nitrogen prior to the photoirradiation experiments. The material was continuously stirred during the course of the experiment. A high power mercury arc lamp 450 W was used as the UV-visible light source for irradiation. The experiment was carried out for 5 h and H₂ evolution was recorded in a time interval of 1 h. Argon was used as the carrier gas. The amount of H₂ produced was measured by gas chromatograph (Shimadzu Gas Chromatograph GC-2010 PLUS) equipped with a molecular sieve column and a TCD detector. The instrument calibration was done prior to the injection.

Results and Discussions

Powder X-ray diffraction studies

The powder X-ray diffraction pattern of the TiO₂ and sodium impregnated TiO₂ materials were shown in Fig. 1. The bare TiO₂ materials showed rutile TiO₂ co-exists with small amounts of anatase phase. The material exhibited diffraction peaks due to d_{101} , d_{004} , d_{200} , and d_{204} at 2θ values of 25, 38, 48 and 62°, respectively, indicative of the anatase phase²². The peaks due to d_{110} , d_{101} , d_{200} , d_{111} , d_{210} , d_{211} , d_{220} , d_{002} , d_{110} , d_{301} , and d_{112} were at 2θ values of 28, 36, 39, 41, 45, 55, 56, 63, 64, 69, and 69°, respectively, indicative of the rutile phase²³. The existence of the mixed phases may be due to partial phase transformation of anatase

to rutile during the calcinations process at 550 °C. Similarly the sodium impregnated TiO₂ showed identical peaks as reported for bare TiO₂ with lower intensities. The crystallinity of TiO₂ anatase and rutile phase was reduced after the formation sodium impregnated TiO₂ as indicated by the reduction in intensities and broadening of the diffraction peaks in this material. A small peak at 31° was present in sodium impregnated sample compared to bare TiO₂ indicated the presence of sodium ion in this material³⁵⁻³⁶.

Raman spectroscopic studies

The Raman spectrum of the sodium impregnated material was shown in Fig. 2, with the inset showing the Raman spectra of bare TiO₂. The bands at 143, 193, 395, 513, and 633 cm⁻¹, are associated with anatase phase of bare TiO₂²². Beside these bands the material showed bands at 450 and 610 cm⁻¹, which were assigned to the rutile phase²³⁻²⁴. The sodium

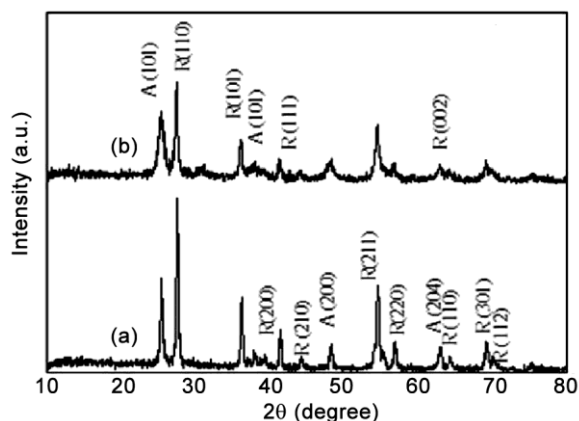


Fig. 1 — Powder XRD pattern of (a) bare TiO₂ and (b) sodium impregnated TiO₂

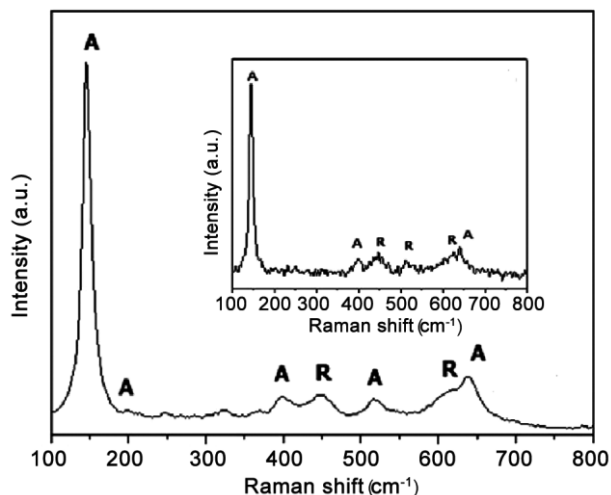


Fig. 2 — Raman spectra of sodium impregnated TiO₂ with the inset showing Raman spectra of bare TiO₂

impregnated TiO₂ material also exhibit identical spectral line. The small peak at 396 cm⁻¹ may be due to the presence of anatase phase in this material.

UV-visible DRS studies

The DRS spectra of TiO₂ and sodium ion impregnated TiO₂ were shown in Fig. 3. Here, the TiO₂ material showed absorption band at 380 nm related to the electronic transition from valence band to conduction band 20 nm and the small absorption edge in the visible region may be due to the presence of rutile phase present in this material. The sodium impregnated TiO₂ material exhibited optical absorption at around 380 nm and a small absorption band at around 400–600 nm range. The intensity of the band at 400–600 nm region was larger than that in bare TiO₂, which may be due to the presence of rutile phase along with sodium ion in this material. It was reported that presence of sodium ion can extend the light absorption to higher wavelength³⁷.

TEM analysis

TEM images of bare TiO₂ and sodium impregnated TiO₂ material are shown in Fig. 4a and Fig. 4b, respectively. TEM images of both materials showed lattice fringes due to TiO₂. The d spacing of 3.25 Å due to (110) associated with rutile phase could be confirmed from TEM image²³.

Photocatalytic water splitting studies

The photocatalytic H₂ evolution results for TiO₂ and sodium impregnated TiO₂ were shown in Fig. 5. The experiments were conducted under UV-visible light using 450 W high pressure Hg arc lamp. The bare TiO₂ material showed an increase in evolution of hydrogen as time goes on. It has been reported that mixed phases TiO₂ can generate hydrogen by photocatalytic splitting of water even in the absence

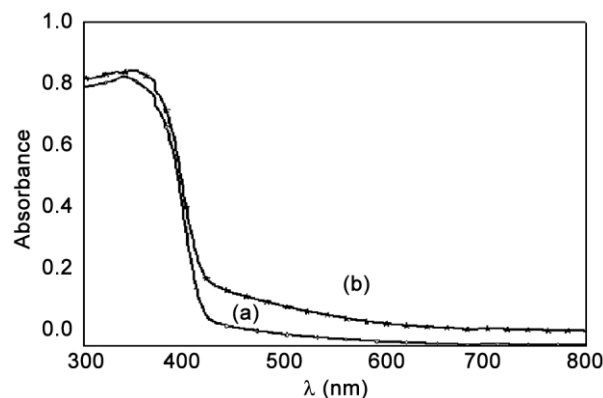


Fig. 3 — Diffuse reflectance UV-visible spectra of (a) TiO₂ and (b) sodium impregnated TiO₂

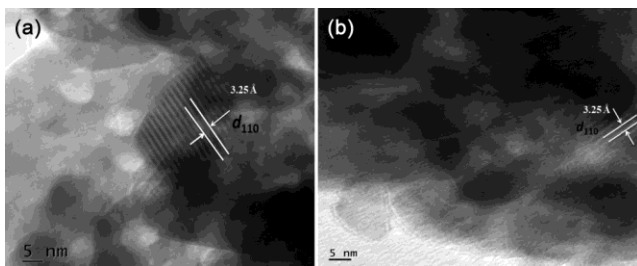


Fig. 4 — TEM image of (a) TiO₂ and (b) sodium impregnated TiO₂

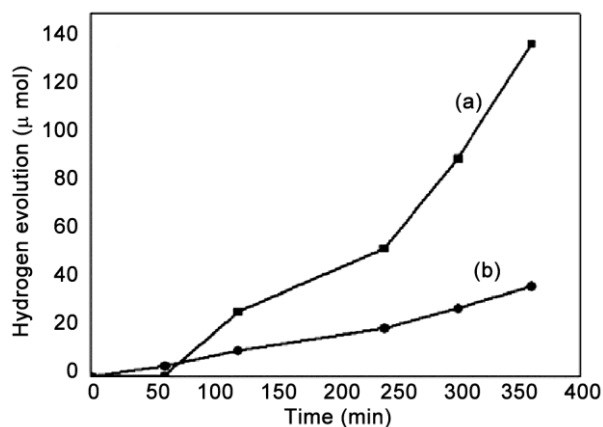


Fig. 5 — Photocatalytic water splitting on (a) bare TiO₂ and (b) sodium impregnated TiO₂nanomaterials

of catalyst promoter³⁸⁻³⁹. The presence of mixed phases of anatase and rutile in bare TiO₂ may minimize charge carrier recombination and generate hydrogen. After 300 min of irradiation the bare TiO₂ material showed H₂ evolution value of 134 μmol. Compared to bare TiO₂ the sodium impregnated TiO₂ nanomaterials showed lower evolution of hydrogen. Even though the presence of anatase/rutile mixed phase TiO₂ may be contributing to the hydrogen evolution in these materials²⁵, the presence of sodium ion⁴⁰⁻⁴³, the poor crystallinity and crystallite size of rutile and anatase phase TiO₂, causing the lower photocatalytic activity of sodium impregnated TiO₂ material compared to bare TiO₂

Conclusions

We prepared photoactive anatase/rutile mixed phase TiO₂ materials by sol gel method. The resultant materials upon modification by impregnation with sodium ions exhibited lower photocatalytic hydrogen under light irradiation. H₂ production achieved from mixed phase TiO₂ was as high as 134 μmol from 0.02 g of catalyst after 5 h of irradiation. However, under similar experimental condition the evolution rate was reduced to a value of 34 μmol. The presence of sodium ion reduces the efficient electron trapping in

shallow states there by reducing the effective separation of the charge carriers and promoting improved photocatalytic water splitting. This work provides information about the detrimental effect of alkali metal ions in solar fuel generation, and for the degradation of organic pollutants.

Acknowledgements

Dr. Parayil acknowledges the financial support of UGC through minor research project grant through 2219-MRP/15- 16/KLCA004/UGC-SWRO and Dr. Resmi acknowledges the financial support of KSCSTE. We are thankful to department of Chemistry, University of Calicut for providing facilities for Raman spectroscopy analysis and M. Akbar at SNGS College Pattambi for water splitting studies.

References

- Bach U, Lupo D, Comte P, Moser J E, Weissörtel F, Salbeck J, Spreitzer H & Grätzel M, *Nature*, 395 (1998) 583.
- Nazeeruddin M K, Humphry-Baker R, Liska P & Grätzel M, *J Phys Chem B*, 107 (2003) 8981.
- Stylidi M, Kondarides D I & Varykios X E, *Appl Catal B*, 47 (2004) 189.
- Hoffmann M R, Martin S T, Choi W & Bahnmann D W, *Chem Rev*, 95 (1995) 69.
- Byrne C, Subramanian G & Pillai S C, *J Environ Chem Eng*, 6 (2018) 3531.
- Moon S-C, Mametsuka H, Tabata S & Suzuki E, *Catal Today*, 58 (2000) 125.
- Noemi L, Ana A S, Elena S, Joaquin S A & Javier G M, *Chem Soc Rev*, 43 (2014) 7681.
- Ran J, Zhang J, Yu J, Jaroniec M & Qiao S Z, *Chem Soc Rev*, 43 (2014) 7787.
- Jang H D, Kim S K, Chang H, Roh K M, Choi J W & Huang J, *Biosens Bioelectron*, 38 (2012) 184.
- Danladi E, Musa G P, Ezra D, *J Energy Nat Res*, 5 (2016) 53.
- Yang C C, Yu Y H, Linden B V D, Wu J C S, Mul G, *J Am Chem Soc*, 132 (2010) 8398.
- Tachibana Y, Hara K, Sayama K & Arakawa H, *Chem Mater*, 14 (2002) 2527.
- Yamakata A, Vequizo J J M & Matsunaga H, *J Phys Chem C*, 119 (2015) 24538.
- Athanasekou C P, Likodimos V & Falaras P, *J Environ Chem Eng*, 6 (2018) 7386.
- Abdullah H, Khan M R, Ong H R & Yaakob Z, *J CO₂ Util*, 22 (2017) 15.
- Wang L, Zhao J, Liu H & Huang J, *J Taiwan Inst Chem Eng*, 93 (2018) 590.
- Lv C, Wang L, Lan X, Yu Q, Zhang M, Sun H & Shi J, *Catal Sci Technol*, 9 (2019) 6124.
- Eidsvåg H, Bentouba S, Vajeeston P, Yohi S & Velauthapillai D, *Molecules*, 26 (2021) 1687.
- Yi S S, Zhang X B, Wulan B R, Yan J M & Jiang Q, *J Energy Environ Sci*, 11 (2018) 3128.
- Xiaohu Z, Tianyou Peng & Shuaishuai Song, *J Mater Chem A*, 4 (2016) 2365.

- 21 Shwetharani R, Sakar M, Fernando C A N, Binas V & Balakrishna R G, *Catal Sci Technol*, 9 (2019) 12
- 22 Parayil S K, Psota R J & Koodali R T, *Int J Hydrogen Energy*, 38 (2013) 10215.
- 23 Parayil S K, Kibombo H S & Koodali R T, *Catal Today*, 199 (2013) 8.
- 24 Parayil S K, Kibombo H S, Wu C M, Peng R, Baltrusaitis J & Koodali R T, *Int J Hydrogen Energy*, 37 (2012) 8257.
- 25 Kho Y K, Iwase A, Teoh W Y, Mädler L, Kudo A & Amal R, *J Phys Chem C*, 114 (2010) 2821.
- 26 Šuligoj A, Arčon I, Mazaj M, Dražić G, Arčon D, Cool P, Štancar U L & Tušar N N, *J Mater Chem A*, 6 (2018) 9882.
- 27 Montoya A T & Gillan E G, *ACS Omega*, 3 (2018) 2947.
- 28 Ola O & Maroto-Valer M, *Appl Catal A: Gen*, 502 (2015) 114.
- 29 Xie H, Li N, Liu B, Yang J & Zhao X, *J Phys Chem C*, 120 (2016), 10390.
- 30 Guillard C, Puzenat E, Lachheb H, Houas A & Herrmann J M, *Int J Photoenergy*, 7 (2009) 1.
- 31 Mironyuk I, Mykytyn I, Vasylyeva H & Savka K, *J Mol Liq*, 316 (2020) Article 113840.
- 32 Shi Z, Yang H, Gao P, Chen X, Liu H, Zhong L, Wang H, Wei W & Sun Y, *Chinese J Catal*, 39 (2018) 1294.
- 33 Nam H J, Amemiya T, Murabayashi M & Itoh K, *Res Chem Intermed*, 31 (2005) 365.
- 34 Prathyusha K R & Sreenivasan K P, *Indian J Chem*, 59A (2020) 747.
- 35 Abdou S M & Moharam H, *J Phys Conf Ser*, 1253 (2019) 012036.
- 36 Addala S, Bouhdjer L, Chala A, Bouhdjar A, Halimi O, Boudine B & Sebais M, *Chinese Phys B*, 22 (2013) 098103.
- 37 Lebukhova N V, Karpovich N F, Pyachin S A, Kirichenko E A, Makarevich K S & Pugachevskii M A, *Theor Found Chem Eng*, 51 (2017) 820.
- 38 Xia X, Peng S, Bao Y, Wang Y, Lei B, Wang Z, Huang Z & Gao Y, *J Power Sources*, 376 (2018) 11.
- 39 AlSalka Y, Hakki A, Schneider J & Bahnemann D W, *Appl Catal B*, 238 (2018) 422.
- 40 Kurtoglu M E, Longenbach T & Gogotsi Y, *Int J Appl Glass Sci*, 2 (2011) 108.
- 41 Rincón A G & Pulgarin C, *Appl Catal B*, 51 (2004) 283.
- 42 Samuel C, Elijah T & Pratim B, *J Electrochem Soc*, 156 (2009) H346.
- 43 Gao X, Guo Q, Tang G, Peng W, Luo Y & He D, *J Water Reuse Desalination*, 9 (2019) 301.